BTS-FR-81-143

NASA CR-166805

FEBRUARY 18, 1981

(NASA-CR-166805) COVARIANCE ANALYSIS OF THE AIRBORNE LASER RANGING SYSTEM Final Report (Business and Technological Systems, Inc.) 42 p HC A03/MF A01 CSCL 20E

N82-25498

Unclas G3/36 21925

COVARIANCE ANALYSIS OF THE AIRBORNE LASER RANGING SYSTEM

FINAL REPORT

BY

THOMAS S. ENGLAR, JR.

CAROL L. HAMMOND

BRUCE P. GIBBS

PREPARED FOR

NATIONAL AERONAUTICS AND SPACE ADMINISTRATION

GODDARD SPACE FLIGHT CENTER

GREENBELT, MARYLAND 20771

BUSINESS AND TECHNOLOGICAL SYSTEMS, INC.

AEROSPACE BUILDING, SUITE 440

SEABROOK, MARYLAND 20801

TABLE OF CONTENTS

1.0 INTRODUCTION

The Airborne Laser Ranging System has been proposed as an effort whereby measurements of the earth's crustal shift can be detected to within centimeters over a region of approximately 200 x 400 km. Hopefully by gaining an understanding of this shift, scientists will be able to more accurately comprehend and predict earthquakes.

Previous analyses have employed spaceborne laser ranging systems. Because of obvious problems arising in the use of spacecraft, this task is devoted to determining the requirements and limitations of employing an airborne system.

Essentially the system consists of an aircraft which flies over a grid of ground deployed retroreflectors. The aircraft flies at two altitudes and presently makes six passes over the grid.

The retroreflector baseline errors are assumed to result from measurement noise, a priori errors on the aircraft and retroreflector positions, tropospheric refraction, and sensor biases.

1.1 Experiment Description

Figure 1.1-1 shows the configuration of the present grid system of retroreflectors. There are currently 15 retros in an area of 40 x 80 km.

The aircraft position is determined by interpolating between the position of the aircraft at the beginning of a pass over the grid and the end of the pass. The aircraft passes start and end 5 km on either side of the grid and the A/C usually flies in the lengthwise direction of the grid at a constant speed of 800 km/hr. Pulses are attempted at a constant time interval.

At each pulse time, a test is performed to select all of the stations in view (those above the 20° elevation cutoff angle), and of

these, the stations upon which measurements will be taken, are chosen. At this point, the sensitivity matrix is computed and the Kalman filter updates are performed.

This process repeats until all passes have been completed. Then the RSS errors are computed in cartesian and baseline coordinates between each station and the master station, which is currently station 1. If at any time, not enough stations are visible, the aircraft simply moves on to the next time.

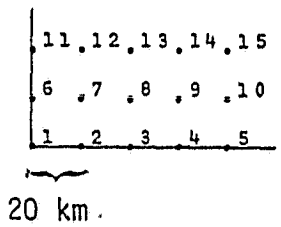

Figure 1.1-1

2.0 Error Analysis

2.1 Error Models

2.1.1 A Priori Station Errors and Constraints

The station positions are assumed to be known in an earth-fixed coordinate system to a level of 100 m (1σ), independent errors in each coordinate direction.

Because the multiple laser measurements from aircraft (geometric measurements) are incapable of determining the global location of this grid, certain station coordinates are assumed to be perfectly known, thus providing the basis for a well-posed problem. The station 1 position is assumed, thus holding the grid in translation. Then the y and z coordinates of station 5 are fixed. This fixes the direction (though not the length) of the 1-5 baseline. In effect, the x-axis of the coordinate system has been defined. Finally, the z component of station 13 is assumed known. These mathematical constraints do not affect the inter-station baseline lengths.

2.1.2 A Priori Aircraft Errors

It is assumed that the A/C position is a gaussian random variable with a standard deviation of 6.3 m in each coordinate direction.

Currently, all runs are made with this error holding every time a pulse is taken. A procedure has been implemented in the Kalman filter for estimating A/C position and velocity in the presence of process noise (see Appendix A). This option, which could significantly improve baseline estimation accuracies at realistic sampling intervals ($\approx$0.2 sec) has not been exercised because it has not been possible to obtain realistic estimates of the process noise variance and time constants.

2.1.3 Measurement Noise and Bias

The laser range measurements are assumed to be corrupted by a bias and a mean-zero, white sequence. The bias is selected from a mean-zero distribution having standard deviation of 1 cm. Each beam has an independent bias and these are solved for in the Kalman filter. The white sequences added to the range measurements are independent on each beam and are gaussian with standard deviation of 1 cm.

2.1.4 Refraction Errors

The model for tropospheric refraction is summarized in [Error Analysis of the Spacelab Geodynamics Laser Ranging System, B. P. Gibbs and E. M. Haley, BTS-TR-78-52, February, 1978]. It appears that the dominant cause of residual refraction error (after range correction for refraction) is errors in the pressure and the gradient of PTK at the retroreflector sites. The procedure hypothesized is to take readings of temperature and pressure at various sites in and around the grid and then fit this data with a polynomial fit to pressure and PTK. This has been done with standard deviations of 1.4° on temperature measurements and 1 mbar on pressure measurements at each of 15 meteorological sites. This data was used to fit pressure and PTK with quadratic polynomials (6 coefficients in each approximation) modeling the horizontal variation and a linear polynomial modeling the horizontal variation of the altitude dependence.

This regression leads to a covariance matrix for errors at the retroreflectors and this is used in the error analysis.

2.2 Sequential Error Analysis

Define:

$\delta a = \hat{x}(0|0) - x(0)$, total error in the prior estimate.

$\delta x(k|\ell) = \hat{x}(k|\ell) - x(k) \qquad k \geq \ell$.

$\delta p = \hat{p} - p$, total error in a set of parameters affecting the measurements.

$\delta x_a(k|\ell) = S_a(k|\ell)\delta a$: Error in estimate caused by error in prior estimate.

$\delta x_v(k|\ell) = S_v(k|\ell)v$: Error in estimate caused by measurement noise.

$\delta x_w(k|\ell) = Sw(k|\ell)w$: Error in estimate caused by process noise.

$\delta x_p(k|\ell) = S_p(k|\ell)\delta p$: Error in estimate caused by parameter errors.

$\delta x(k|\ell) = \delta x_a + \delta x_v + \delta x_w + \delta x_p$

$\tilde{x}(k|\ell)$: Error in estimate caused by modeled effects. In the ABLRS $\tilde{x} = \delta x_a + \delta x_v + \delta x_w$.

Let us suppose that we have measurements $\{z_k\}$, k=1, ··· ,

$$z_k = H(k)x(k) + B(k)\delta p + v_k ,$$

and an estimate $\hat{x}(\ell|\ell)$ of $x(\ell)$ based on $\{z_k\}^{\ell}$, and $\hat{x}(0|0)$. Then

$$\delta x(\ell|\ell) = \tilde{x}(\ell|\ell) + S_p(\ell|\ell)\delta p \ .$$

The propagation of $x(\ell)$ is given by

$$x(\ell+1) = \phi x(\ell) + u(\ell) \ ,$$

where

$$Eu(\ell) = 0$$
$$Eu(\ell)u(k) = Q\delta_{\ell k} \ .$$

Therefore,

$$\hat{x}(\ell+1|\ell) = \phi\hat{x}(\ell|\ell)$$

so that

$$S_p(\ell+1|\ell) = \phi S_p(\ell|\ell)$$

and

$$P(\ell+1|\ell) = E\tilde{x}(\ell+1|\ell)\tilde{x}^T(\ell+1|\ell) = \phi P(\ell|\ell)\phi^T + Q \ .$$

Now when a measurement update takes place,

$$\hat{x}(\ell+1|\ell+1) = \hat{x}(\ell+1|\ell) + K(z_{\ell+1} - H\hat{x}(\ell+1|\ell)) \ ,$$

then

$$\delta x(\ell+1|\ell+1) = \delta x(\ell+1|\ell) - KH\delta x(\ell+1|\ell)$$
$$+ KB\delta p + Kv \ ,$$
$$= (I-KH)[\tilde{x}(\ell+1|\ell) + S_p(\ell+1|\ell)\delta p]$$
$$+ KB\delta p + Kv \ .$$

Using this, we can calculate that

$$P(\ell+1|\ell+1) = (I-KH)P(\ell+1|\ell)(I-KH)^T + KRK^T$$

and

$$S_p(\ell+1|\ell+1) = (I-KH)S_p(\ell+1|\ell) + KB \ .$$

To obtain these results, we have assumed that δa , v_k , w_k and δp are uncorrelated random variables.

Finally, the errors caused by the unadjusted parameters, δp , are obtained from

$$P_\delta = S_p(T|T)E\{\delta p \delta p^T\}S_p^T(T|T) \ .$$

3.0 RESULTS

The results presented in this section have all been obtained from computer runs implementing a 15 station grid. In base run the stations were placed in a 40 x 80 km area, with 20 km separation. In subsequent runs, grid size was varied, and the results of this variation will be discussed later in this section. We have concentrated on ten specific effects and each is described separately. Tables have been included as an aid to understanding the results. A brief explanation of the tables follows.

The first column of each table contains the station coordinates in the baseline system. In this system, the axes are different for each station. One axis is defined as the vector between the reference station, or master station, and a given station. In all of our examples, station 1 is the master station. The component along this axis is the "along" baseline component, or the "L" component. Perpendicular to this axis in the ground plane is the second axis, where the cross component, or "C" component, is measured. Orthogonal to these axes in the vertical direction, is the height, or "H" component. Thus, the L_2 notation, for example, means the along baseline component between station 2 and the master station.

Also in the first column are the system biases associated with laser beams 1 through the number of beams.

The recovery errors listed in the tables are in units of centimeters. A zero in any component of a station signifies that a coordinate system constraint was placed on that component. Coordinate system constraints are discussed in Section 2.1.1 of this report.

To the side of the table, other pertinent information is listed. The number of measurements is given where measurement is taken to mean the number of aircraft positions or the number of laser pulses. The

actual number of measurements is this number times the number of beams. Also given is the number of beams, the time increment between pulses, and the aircraft low altitude.

3.1 Aircraft Altitude and Flight Path

One of the first priorities in the study is to determine optimal aircraft altitude and flight path. Early studies showed that it is necessary to fly the aircraft at more than one altitude in order to achieve good station recovery, especially in the "height" component. Two altitudes seem to be sufficient in providing the necessary geometry for acceptable recovery. The high altitude has been chosen as 19 km, which is near the maximum ceiling of the aircraft. The aircraft flies faster and for longer periods of time at higher altitudes - two desirable traits in a time and cost limited mission. The low altitude controls retro-reflector separation - the lower the aircraft, the closer the stations. Accuracy is improved at low altitudes. Several computer runs have been made varying the low altitude of the aircraft to compute sensitivities.

Table 1 shows the comparison between low altitudes of 11, 13 and 15 km, with station separation of 20 km. If the results are compared directly, the picture is very confusing. Consider the 11 km and 13 km results for instance. For baselines closer than 45° to the flight path results are improved at the higher altitude. This is anomalous for two reasons: first, we anticipate that distance accuracy should be isotropic; second, we expect errors to increase as altitude separation decreases. The primary suspect for lack of symmetry is the flight path arrangement, particularly the lack of any A/C positions outside the long boundaries of the grid.

While the higher altitude has more measurements (13 km has 440) than the lower altitude (11 km has 370), the improvement seems to be somewhat better than could be expected on this basis alone. We hypothesize that

this may be because of the increased number of measurements outside the grid.

In comparing the results of the 15 km run with both the 11 km and 13 km results, it is obvious that accuracy is lost as the two aircraft passes are placed closer together.

The aircraft flies three passes at the low altitude and three passes at the high altitude. It is planned that these passes should be directly over the line of retros. However, the low pass over the boundary line has some difficulty in seeing six stations at all times. For this reason, the low passes over the boundaries were moved inside the grid. Results showed, however, that good viewing geometry depended strongly upon construction of a viewing triangle over the grid, requiring that the passes lie in a plane containing the retros. Therefore, both the upper and lower passes were moved inside, as shown in Figure 3.1-1. Table 2 shows the comparison between flying directly over the retro line and flying inside the boundaries. In general, recovery is improved when flying inside and the improvement is probably caused by the increased number of measurements.

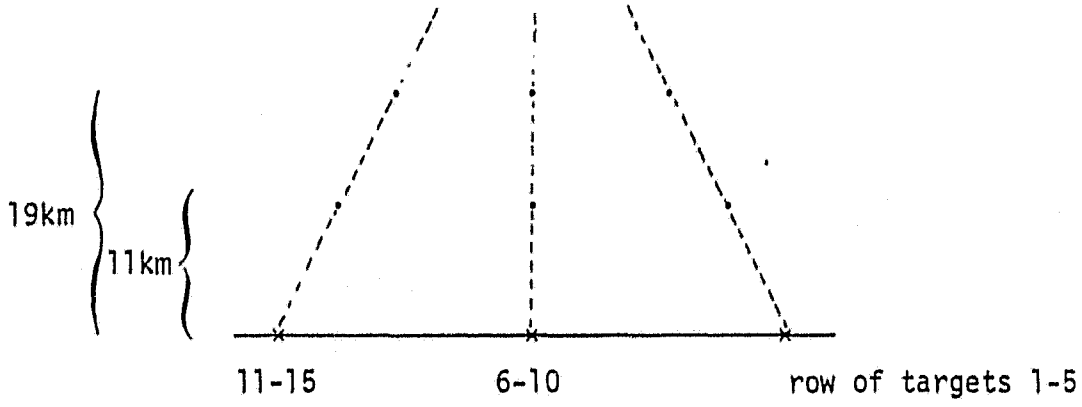

Figure 3.1-1 Crossection

3.2 Retro Separation

The problem of retro separation is closely related to A/C altitude. At low altitudes, the retros must be closer together. Otherwise, visibility problems occur. Costwise, fewer stations placed farther apart are desirable. In Table 3, a comparison is made between two runs different only in the retro separation. In both runs, the low A/C altitude was 15 km. In the first run the retros were 27.27 km apart (the largest acceptable separation) and in the second, they were 20 km apart. The results show clearly that the interstation baselines are more accurately determined with the smaller spacing. However, it appears that the error in determining a given baseline length, e.g., 80 km, is independent of station spacing.

Examination of Tables 1 and 3 in the light of this observation indicates that a careful evaluation of A/C low altitude between 11 km and 15 km, together with maximized retro spacing may produce an optimized cost for a given area. This will be studied in the near future.

3.3 Number of Beams

Another area of interest is the effect of varying the number of beams on board the A/C and varying the minimum number of retros that must be visible at each time for measurement processing to occur. Table 4 shows the results of this testing.

In column 1, the base run, 6 beams were employed along with the criterion that at least 6 retros must be visible at all times. In this run 185 A/C positions were used. In comparing these results with column 2, where there were 7 beams/6 required (185 A/C positions), we see that the results were somewhat better with seven beams - but improvements were less than 9% in baseline and generally less at long distances. In fact, baselines 11, 12 and 13 deteriorated slightly, apparently a numerical problem. Improvement was uniform in height and cross.

In column 3, where there were 7 beams/7 required (150 A/C positions) results were worse. This is attributed to the fact that very few measurements were taken at the low altitude because of severe visibility problems.

In column 4 (216 A/C positions) with 5 beams/5 visible there was considerable degradation, as much as 30% on baselines 6 and 11. While this distinctive change in the 1, 6, 11 boundary is probably somehow caused by the "choose" algorithm, it is fairly clear that the five beam possibility is used at considerable cost in accuracy.

Finally, column 5 employed 6 beams/5 visible. In this run, 216 A/C positions were used, and results were uniformly improved in baseline, cross and height components. Although the improvements were not great (generally 5-8%), the addition of these extra measurements was made with very little extra computational burden.

3.4 Choose Algorithm

The problem arises, when more stations are visible than there are beams, of which stations to choose to take measurements on. Tests have been performed on two methods of choosing these stations. In method 1, the criterion for selection is distance from the A/C to the retro. Presently, we choose the 2 closest and 4 farthest retros in the 6 beam case. Method 2 utilizes a random choose algorithm.

Contrary to initial speculation, using the random choose algorithm in the base run produced slightly less accurate results in all baselines except 7 and 12. The reason for this is not known and is thought to be numerical. These results may be seen in the first 2 columns of Table 5.

In the five beam case (columns 4, 5 of Table 5) a majority of the baseline recoveries were better using the random choose algorithm, especially the longer baselines. The cross component of the longer

baselines seemed to improve with the random choose process, some as much as 13%. The height component of the interior retros improved with the random choose, while the height recovery of the border retros deteriorated with that method.

Additional runs to see what benefit is obtained from using random choose will be performed.

The 2 closest, 4 farthest criterion was originally chosen in an attempt to maximize geometric strength. Two characteristics of this procedure led to the random algorithm. First, the closest always went to beam #1, which we thought led to the poorer determination of bias one. Inasmuch as the random choose corrects this inequality, the procedure is effective. However, there is no significant improvement of the baseline recovery. Second, in a time interval when more than six stations are visible, the deterministic procedure will always select the same stations. It seemed that taking different combinations of stations might strengthen the solution.

It appears, however, that any algorithm which takes both near and far stations will produce quite similar results.

In an effort to support the theory of needing both close and far stations, a computer run was made where the 6 closest stations were always chosen. The results of this run can be seen in column 3 of Table 5. Clearly, the baseline recoveries have suffered as a result of poor geometry.

3.5 Basic Measurement Noise Variance Versus Number of Measurements

Computational burden is greatly increased by a decrease in time between measurements. When the Δt is halved, central processing unit time is doubled. For this reason, we were interested in performing tests to find out if a large number of measurements could be simulated by using

a smaller basic measurement noise variance. The results of this test can be seen in Table 6 where the baseline errors are virtually identical. In column 1 these errors were achieved using a $\Delta t = 2.5$ and a basic measurement noise variance = 1. In column 2, $\Delta t = 5.0$ and the basic measurement noise variance = 0.5.

It is interesting to note in Table 7, columns 1, 2, 3 (Δt = 10, 5, 2.5) that behavior of the cross component is very well described by $N^{-1/2}$. This same behavior is shown in columns 4 through 8 (measurement $\sigma \approx$ 1.414, 1.0, 0.707, 0.5, 0.3). We see also that halving Δt is equivalent to halving measurement noise variance.

This indicates that the observability problem, or a priori influence, which strongly affects baseline and height is not impacting the cross component.

3.6 A Priori Variance

In Table 8 we decreased the a priori variance on the bias. In column 1 the variance was 1, in column 2 the variance was 0.25 and in column 3 the variance was 0.09. These runs indicate that prior information on bias is still strongly affecting height and baseline recovery. The cross component, however, is independent of bias. Previous runs have shown that recovery is independent of prior data on station and A/C - at least while that prior is at the 10m - 30m level.

These results are consistent with those in Table 7 indicating that the cross component is noise limited and independent of bias. In order to determine whether the difficulties in reaching the noise-limited condition are because of marginal observability or the influence of prior data, two runs were made with large prior variances on bias. These runs, column 4 (σbias = 1000 cm) and column 5 (σbias = 500 cm), show that results are independent of prior variances when the biases are much larger than the posterior estimates. This indicates that the system is

completely observable. However, it does not tell us when the system becomes noise limited. In order to determine how large numbers of measurements will affect the recovery, the simplest procedure is to decrease the measurement noise and properly adjust the process noise.

3.7 Effect of Process Noise

The results presented in the previous sections have all assumed A/C position uncertainty of 9.5 m in each axis at each measurement point. Since the position of the A/C must be solved for and the uncertainty cannot grow to this magnitude in the 0.1 - 0.2 second interval between "shots", this uncertainty induces a very pessimistic estimate of recovery errors. To provide a realistic evaluation, a process noise simulation has been implemented and is described in Appendix A. In order to check the implementation, unreasonably large values were used. These results are shown in Table 9.

An estimate of how large the uncertainties should be is difficult to obtain. However, using the parameters described in Appendix A and a 10 sec measurement interval, there is no improvement. However, if the interval were reduced, as it is in the operational system, improvement would show. It is difficult to evaluate this properly without actually running at 0.2 sec. however, which is financially prohibitive.

In the operational data reduction, the process noise can be evaluated, of course, so as to close the loop on the numerical values.

3.8 Refraction

Since refraction is a very important error source, it is necessary to consider its contribution to the errors in baseline recovery. Table 11, column 2 shows our first attempt at refraction in the "consider" mode. The noise only errors are identical to the base run errors in column 1. The unadjusted errors are all less than 0.7 cm. Column 3

shows the results of the same run when the random choose algorithm is selected. The noise only baseline errors exhibit the same characteristics as previously discussed, while the unadjusted errors show "random" improvement throughout the grid. Column 5 shows the results when the time increment between measurements was reduced to 5 sec. The noise only errors are identical to the errors in the base run for $\Delta t = 5$ sec. (column 4).

3.9 Cross Passes

Four cross passes were added to the A/C flight path to see if the geometry would be improved enough for significant reductions in the baseline recoveries. The results in Table 12 show that the baseline component errors were slightly better than would have been expected given the additional number of measurements and that the height component errors were very close to the expected errors.

Therefore, it seems that there is no pronounced improvement in recoveries as a result of adding cross passes to the flight plan.

3.10 Operational Projections

From Table 11, an accurate estimate of refraction errors is obtained. From Table 7, the evolution of error can be traced as Δt becomes smaller, and it appears that each halving of Δt is accompanied by an error reduction of about 15%. This reduction is applied six times to obtain the equivalent of a pulse interval of 0.156 sec. Although the laser pulses every 0.1 sec we anticipate a 33% signal loss and thus 0.15 sec seems a reasonable data interval. These results are multiplied by $\sqrt{2}$ (to simulate the errors in baseline change obtained from two experiments) and are shown in Figure 3.10-1.

In Figure 3.10-2 the analogous baseline rate accuracy is shown.

While larger grids have not been tested, these results will hold for the same size subsections of larger grids, provided the number of measurements and the geometry is preserved.

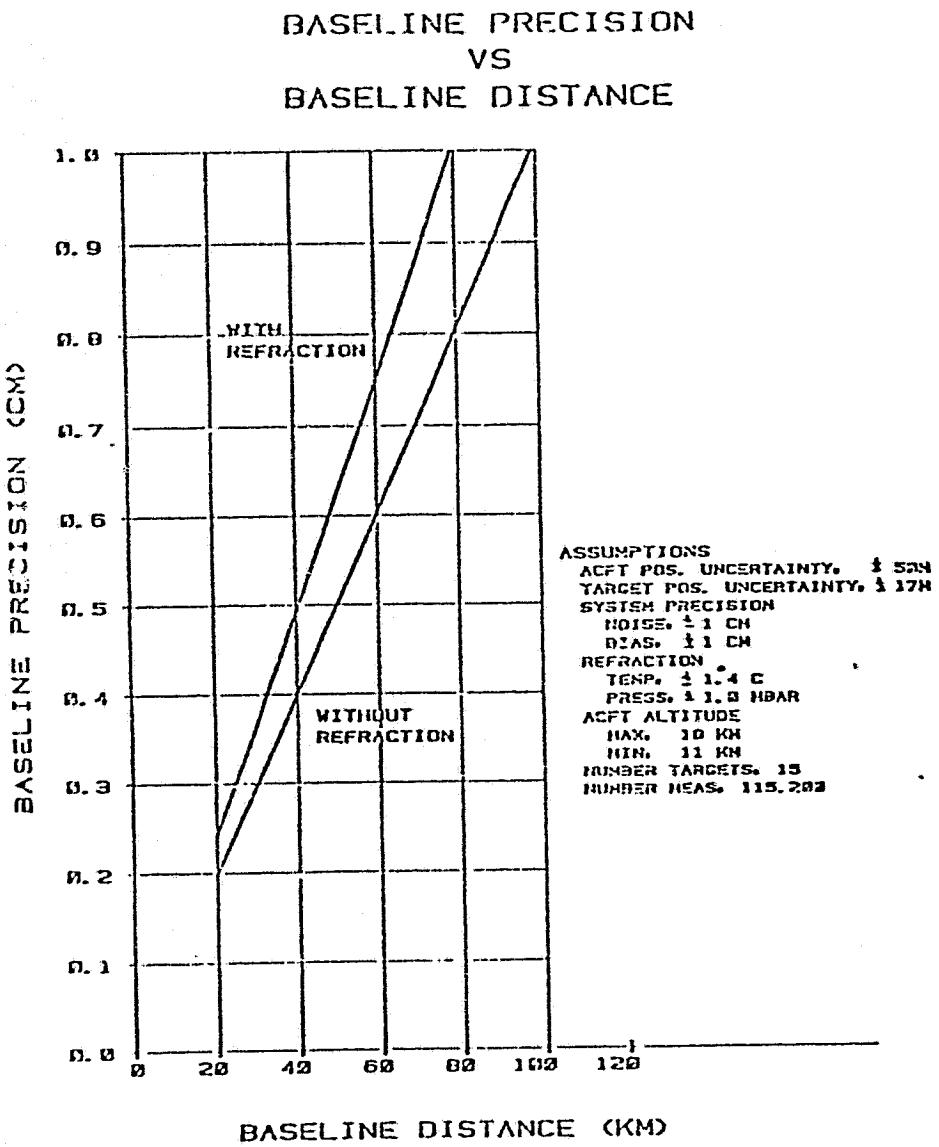

Figure 3.10-1

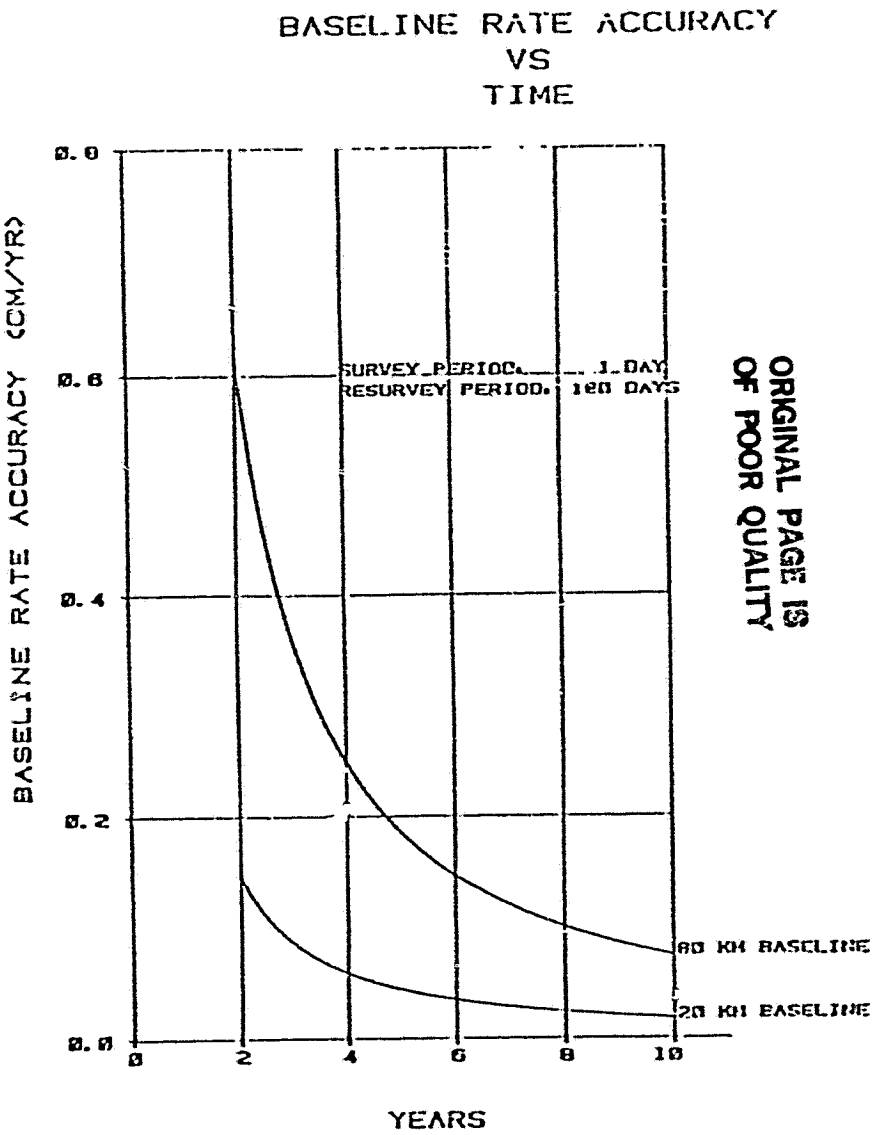

Figure 3.10-2

Table 1 - Low Altitude Variation

		11 km.	13 km.	15 km.
Stations	H2	1.16	1.09	1.36
	L2	0.59	0.53	0.58
	C2	0.36	0.38	0.32
	H3	1.47	1.38	1.76
	L3	0.91	0.38	0.96
	C3	0.36	0.37	0.35
	H4	1.17	1.09	1.36
	L4	1.28	1.15	1.35
	C4	0.39	0.39	0.32
	H5	0.00	0.00	0.00
	L5	1.68	1.50	1.80
	C5	0.00	0.00	0.00
	H6	1.15	1.29	1.65
	L6	0.61	0.69	0.80
	C6	0.52	0.52	0.60
	H7	0.80	0.87	1.06
	L7	0.73	0.75	0.83
	C7	0.53	0.57	0.75
	H8	0.91	0.92	1.17
	L8	0.97	0.92	1.05
	C8	0.56	0.65	0.83
	H9	0.82	0.93	1.15
	L9	1.28	1.16	1.38
	C9	0.59	0.69	0.86
	H10	1.14	1.29	1.65
	L10	1.65	1.48	1.78
	C10	0.61	0.73	0.88
	H11	2.11	2.20	2.83
	L11	0.94	1.19	1.47
	C11	0.86	0.88	1.06
	H12	0.89	0.95	1.18
	L12	0.99	1.16	1.40
	C12	0.81	0.92	1.19
	H13	0.00	0.00	0.00
	L13	1.15	1.20	1.41
	C13	0.85	1.05	1.38
	H14	0.87	0.92	1.14
	L14	1.42	1.36	1.58
	C14	0.88	1.14	1.49
	H15	2.04	2.10	2.66
	L15	1.75	1.63	1.92
	C15	0.93	1.17	1.56
Biases	1	0.40	0.38	0.43
	2	0.37	0.36	0.39
	3	0.39	0.38	0.39
	4	0.39	0.37	0.39
	5	0.38	0.37	0.38
	6	0.37	0.36	0.37

6 Beams

Δt = 5. sec.

Column	Number of Measurements Per Beam
1	370
2	440
3	476

Table 2 - Variation in Aircraft Flight Path

		Directly Over	Inside
Stations	H2	1.55	1.51
	L2	0.80	0.77
	C2	0.44	0.51
	H3	1.99	1.89
	L3	1.19	1.13
	C3	0.49	0.51
	H4	1.56	1.53
	L4	1.65	1.55
	C4	0.45	0.55
	H5	0.00	0.00
	L5	2.16	2.05
	C5	0.00	0.00
	H6	1.74	1.62
	L6	0.84	0.82
	C6	0.77	0.73
	H7	1.13	1.07
	L7	1.04	0.95
	C7	0.82	0.75
	H8	1.22	1.15
	L8	1.27	1.20
	C8	0.90	0.79
	H9	1.18	1.11
	L9	1.63	1.54
	C9	0.97	0.83
	H10	1.72	1.60
	L10	2.08	1.98
	C10	0.95	0.87
	H11	3.02	2.88
	L11	1.26	1.23
	C11	1.24	1.20
	H12	1.26	1.24
	L12	1.31	1.28
	C12	1.18	1.13
	H13	0.00	0.00
	L13	1.47	1.43
	C13	1.25	1.21
	H14	1.21	1.21
	L14	1.76	1.70
	C14	1.32	1.25
	H15	2.84	2.76
	L15	2.17	2.08
	C15	1.38	1.32
Biases	1	0.43	0.43
	2	0.39	0.40
	3	0.42	0.42
	4	0.42	0.41
	5	0.40	0.40
	6	0.40	0.39

Low Altitude = 11 km.

6 Beams

Δt = 10 sec.

Column	Number of Measurements Per Beam
1	177
2	185

Table 3 - Retroreflector Separation Variation

		27.27 km Separation	20 km Separation
Stations	H2	2.38	1.36
	L2	0.77	0.58
	C2	0.42	0.32
	H3	3.15	1.76
	L3	1.31	0.96
	C3	0.51	0.35
	H4	2.40	1.36
	L4	1.83	1.35
	C4	0.45	0.32
	H5	0.00	0.00
	L5	2.38	1.80
	C5	0.00	0.00
	H6	2.53	1.65
	L6	0.82	0.80
	C6	0.77	0.60
	H7	1.52	1.06
	L7	1.00	0.83
	C7	0.80	0.75
	H8	1.73	1.17
	L8	1.38	1.05
	C8	0.89	0.83
	H9	1.59	1.15
	L9	1.81	1.38
	C9	0.91	0.86
	H10	2.69	1.65
	L10	2.33	1.78
	C10	0.94	0.88
	H11	4.62	2.83
	L11	1.44	1.47
	C11	1.38	1.06
	H12	1.92	1.18
	L12	1.45	1.40
	C12	1.37	1.19
	H13	0.00	0.00
	L13	1.60	1.41
	C13	1.48	1.38
	H14	1.95	1.14
	L14	1.94	1.58
	C14	1.59	1.49
	H15	4.64	2.66
	L15	2.41	1.92
	C15	1.68	1.56
Biases	1	0.38	0.43
	2	0.35	0.39
	3	0.37	0.39
	4	0.36	0.39
	5	0.34	0.38
	6	0.34	0.37

Low Altitude = 15 km.

6 Beams

Δt = 5 sec.

Column	Number of Measurements Per Beam
1	471
2	476

Table 4 - Variation in Number of Beams

		6 beams 6 visible	7 beams 6 visible	7 beams 7 visible	5 beams 5 visible	6 beams 5 visible
Stations	H2	1.51	1.41	1.68	1.58	1.39
	L2	0.77	0.71	0.83	0.85	0.72
	C2	0.51	0.46	0.51	0.71	0.50
	H3	1.89	1.77	2.16	1.95	1.73
	L3	1.13	1.04	1.26	1.19	1.04
	C3	0.51	0.49	0.52	0.70	0.50
	H4	1.53	1.42	1.69	1.58	1.40
	L4	1.55	1.42	1.73	1.63	1.42
	C4	0.55	0.46	0.52	0.81	0.54
	H5	0.00	0.00	0.00	0.00	0.00
	L5	2.05	1.87	2.28	2.12	1.86
	C5	0.00	0.00	0.00	0.00	0.00
	H6	1.62	1.59	1.86	1.81	1.50
	L6	0.82	0.79	0.92	1.06	0.79
	C6	0.73	0.70	0.81	0.86	0.70
	H7	1.07	1.12	1.18	1.26	1.05
	L7	0.95	0.91	0.97	1.09	0.92
	C7	0.75	0.68	0.92	0.89	0.70
	H8	1.15	1.15	1.30	1.35	1.10
	L8	1.20	1.16	1.33	1.33	1.14
	C8	0.79	0.74	0.97	0.97	0.74
	H9	1.11	1.01	1.18	1.41	1.07
	L9	1.54	1.46	1.73	1.68	1.45
	C9	0.83	0.78	0.98	1.05	0.78
	H10	1.60	1.48	1.83	1.92	1.53
	L10	1.98	1.85	2.23	2.12	1.84
	C10	0.87	0.87	1.02	1.19	0.83
	H11	2.88	2.65	3.32	3.27	2.65
	L11	1.23	1.24	1.38	1.65	1.21
	C11	1.20	1.14	1.35	1.41	1.15
	H12	1.24	1.16	1.43	1.46	1.16
	L12	1.28	1.30	1.37	1.63	1.26
	C12	1.13	1.04	1.36	1.43	1.09
	H13	0.00	0.00	0.00	0.00	0.00
	L13	1.43	1.44	1.54	1.70	1.40
	C13	1.21	1.10	1.46	1.54	1.14
	H14	1.21	1.19	1.46	1.42	1.15
	L14	1.70	1.67	1.88	1.96	1.63
	C14	1.25	1.17	1.54	1.64	1.19
	H15	2.76	2.70	3.28	3.16	2.62
	L15	2.08	2.01	2.33	2.33	1.97
	C15	1.32	1.26	1.66	1.74	1.24
Biases	1	0.43	0.41	0.43	0.49	0.42
	2	0.40	0.38	0.39	0.44	0.40
	3	0.42	0.39	0.41	0.48	0.41
	4	0.41	0.38	0.39	0.45	0.40
	5	0.40	0.37	0.38	0.45	0.39
	6	0.39	0.37	0.38	-	0.39
	7	-	0.36	0.37	-	-

Low Altitude = 11 km.

Δt = 10. sec.

Column	Number of Measurements Per Beam
1	185
2	185
3	150
4	216
5	216

Table 5 - Choose Algorithm Comparison

		2 Closest 4 Farthest	Random	6 Closest	2 Closest 4 Farthest	Random
Stations	H2	1.51	1.62	2.09	1.58	1.72
	L2	0.77	0.79	1.00	0.85	0.84
	C2	0.51	0.54	0.68	0.71	0.66
	H3	1.89	2.03	2.73	1.95	2.15
	L3	1.13	1.17	1.50	1.19	1.23
	C3	0.51	0.59	0.78	0.70	0.74
	H4	1.53	1.67	2.05	1.58	1.73
	L4	1.55	1.58	1.84	1.63	1.60
	C4	0.55	0.57	0.64	0.81	0.66
	H5	0.00	0.00	0.00	0.00	0.00
	L5	2.05	2.08	2.31	2.12	2.10
	C5	0.00	0.00	0.00	0.00	0.00
	H6	1.62	1.62	1.82	1.81	1.83
	L6	0.82	0.82	0.81	1.06	0.93
	C6	0.73	0.78	0.92	0.86	0.90
	H7	1.07	1.06	1.42	1.26	1.26
	L7	0.95	0.92	1.19	1.09	1.09
	C7	0.75	0.74	0.87	0.89	0.81
	H8	1.15	1.22	1.66	1.35	1.34
	L8	1.20	1.25	1.56	1.33	1.34
	C8	0.79	0.79	0.95	0.97	0.86
	H9	1.11	1.13	1.28	1.41	1.30
	L9	1.54	1.60	1.87	1.68	1.66
	C9	0.83	0.80	0.93	1.05	0.90
	H10	1.60	1.69	1.95	1.92	1.89
	L10	1.98	2.06	2.31	2.12	2.09
	C10	0.87	0.86	0.98	1.19	0.98
	H11	2.88	3.00	3.38	3.27	3.31
	L11	1.23	1.27	1.40	1.65	1.57
	C11	1.20	1.23	1.45	1.41	1.37
	H12	1.24	1.35	1.51	1.46	1.51
	L12	1.28	1.25	1.44	1.63	1.47
	C12	1.13	1.20	1.32	1.43	1.28
	H13	0.00	0.00	0.00	0.00	0.00
	L13	1.43	1.46	1.71	1.70	1.65
	C13	1.21	1.26	1.36	1.54	1.34
	H14	1.21	1.34	1.66	1.42	1.46
	L14	1.70	1.77	2.06	1.96	1.88
	C14	1.25	1.28	1.38	1.64	1.42
	H15	2.76	3.10	3.86	3.16	3.25
	L15	2.08	2.21	2.51	2.33	2.27
	C15	1.32	1.38	1.56	1.74	1.55
Biases	1	0.43	0.39	0.44	0.49	0.43
	2	0.40	0.38	0.40	0.44	0.42
	3	0.42	0.39	0.40	0.48	0.43
	4	0.41	0.39	0.40	0.45	0.43
	5	0.40	0.39	0.41	0.45	0.43
	6	0.39	0.39	0.43	-	-

Low Altitude = 11 km.

Δt = 10. sec.

Col. 1-3 = 6 beams

Col. 4-5 = 5 beams

Column	Number of Measurements Per Beam
1	185
2	185
3	185
4	216
5	216

Table 6 - Basic Measurement Noise Variance

		Δt = 2.5 Variance=1.	Δt = 5. Variance=0.5
Stations	H2	0.90	0.91
	L2	0.46	0.46
	C2	0.26	0.26
	H3	1.16	1.17
	L3	0.75	0.75
	C3	0.26	0.26
	H4	0.91	0.92
	L4	1.06	1.07
	C4	0.27	0.27
	H5	0.00	0.00
	L5	1.40	1.42
	C5	0.00	0.00
	H6	0.83	0.84
	L6	0.46	0.46
	C6	0.37	0.37
	H7	0.61	0.61
	L7	0.58	0.58
	C7	0.38	0.38
	H8	0.74	0.74
	L8	0.81	0.81
	C8	0.39	0.40
	H9	0.63	0.63
	L9	1.07	1.08
	C9	0.41	0.42
	H10	0.82	0.82
	L10	1.39	1.41
	C10	0.43	0.43
	H11	1.57	1.59
	L11	0.74	0.75
	C11	0.60	0.61
	H12	0.64	0.64
	L12	0.79	0.80
	C12	0.57	0.57
	H13	0.00	0.00
	L13	0.95	0.96
	C13	0.60	0.61
	H14	0.63	0.63
	L14	1.19	1.20
	C14	0.62	0.62
	H15	1.53	1.54
	L15	1.48	1.49
	C15	0.66	0.66
Biases	1	0.36	0.36
	2	0.34	0.34
	3	0.36	0.36
	4	0.35	0.35
	5	0.34	0.35
	6	0.34	0.34

Low Altitude = 11 km.

6 Beams

Column	Number of Measurements Per Beam
1	738
2	370

Table 7

		Δt=10.	Δt=5.	Δt=2.5	meas. σ = 1.414	meas. σ = 1.	meas. σ = .707	meas. σ = .5	meas. σ = .3
Stations	H2	1.51	1.16	0.90	1.51	1.16	0.91	0.72	0.50
	L2	0.77	0.59	0.46	0.78	0.59	0.46	0.36	0.25
	C2	0.51	0.36	0.26	0.51	0.36	0.26	0.18	0.11
	H3	1.89	1.47	1.16	1.89	1.47	1.17	0.94	0.65
	L3	1.13	0.91	0.75	1.13	0.91	0.75	0.62	0.44
	C3	0.51	0.36	0.26	0.51	0.36	0.26	0.18	0.11
	H4	1.53	1.17	0.91	1.52	1.17	0.92	0.73	0.50
	L4	1.55	1.28	1.06	1.55	1.28	1.07	0.89	0.64
	C4	0.55	0.39	0.27	0.55	0.39	0.27	0.19	0.12
	H5	0.00	0.00	0.00	0.00	0.00	0.00	0.00	0.00
	L5	2.05	1.68	1.40	2.04	1.68	1.42	1.19	0.86
	C5	0.00	0.00	0.00	0.00	0.00	0.00	0.00	0.00
	H6	1.62	1.15	0.83	1.61	1.15	0.84	0.61	0.38
	L6	0.82	0.61	0.46	0.82	0.61	0.46	0.35	0.24
	C6	0.73	0.52	0.37	0.73	0.52	0.37	0.26	0.16
	H7	1.07	0.80	0.61	1.06	0.80	0.61	0.47	0.32
	L7	0.95	0.73	0.58	0.95	0.73	0.58	0.46	0.32
	C7	0.75	0.53	0.38	0.75	0.53	0.38	0.27	0.16
	H8	1.15	0.91	0.74	1.15	0.91	0.74	0.60	0.43
	L8	1.20	0.97	0.81	1.20	0.97	0.81	0.67	0.48
	C8	0.79	0.56	0.39	0.79	0.56	0.40	0.28	0.17
	H9	1.11	0.82	0.63	1.10	0.82	0.63	0.49	0.33
	L9	1.54	1.28	1.07	1.55	1.28	1.08	0.91	0.66
	C9	0.83	0.59	0.41	0.83	0.59	0.42	0.30	0.18
	H10	1.60	1.14	0.82	1.59	1.14	0.82	0.60	0.37
	L10	1.98	1.65	1.39	1.98	1.65	1.41	1.18	0.86
	C10	0.87	0.61	0.43	0.87	0.61	0.43	0.31	0.19
	H11	2.88	2.11	1.57	2.85	2.11	1.59	1.21	0.80
	L11	1.23	0.94	0.74	1.22	0.94	0.75	0.59	0.41
	C11	1.20	0.86	0.60	1.21	0.86	0.61	0.43	0.26
	H12	1.24	0.89	0.64	1.24	0.89	0.64	0.47	0.29
	L12	1.28	0.99	0.79	1.27	0.99	0.80	0.64	0.45
	C12	1.13	0.81	0.57	1.14	0.81	0.57	0.40	0.24
	H13	0.00	0.00	0.00	0.00	0.00	0.00	0.00	0.00
	L13	1.43	1.15	0.95	1.43	1.15	0.96	0.79	0.57
	C13	1.21	0.85	0.60	1.21	0.85	0.61	0.43	0.26
	H14	1.21	0.87	0.63	1.21	0.87	0.63	0.46	0.29
	L14	1.70	1.42	1.19	1.71	1.42	1.20	1.01	0.73
	C14	1.25	0.88	0.62	1.24	0.88	0.62	0.44	0.27
	H15	2.76	2.04	1.53	2.76	2.04	1.54	1.17	0.77
	L15	2.08	1.75	1.48	2.09	1.75	1.49	1.25	0.91
	C15	1.32	0.93	0.66	1.31	0.93	0.66	0.47	0.28
Biases	1	0.43	0.40	0.36	0.43	0.40	0.36	0.32	0.24
	2	0.40	0.37	0.34	0.40	0.37	0.34	0.30	0.22
	3	0.42	0.39	0.36	0.42	0.39	0.36	0.32	0.24
	4	0.41	0.39	0.35	0.41	0.39	0.35	0.31	0.23
	5	0.40	0.38	0.34	0.40	0.38	0.35	0.30	0.23
	6	0.39	0.37	0.34	0.39	0.37	0.34	0.30	0.22

Low Altitude = 11 km

6 Beams

Δt = 5. sec.
(Col. 4-8)

Column	Number of Measurements Per Beam
1	185
2	370
3	738
4	370
5	370
6	370
7	370
8	370

Table 8 - A Priori Variance on Bias

		Variance = 1.	Variance = .25	Variance = .09	σ = 1000 cm.	σ = 500 cm.
Stations	H2	1.16	1.01	0.97	2.71	2.71
	L2	0.59	0.53	0.51	1.34	1.34
	C2	0.36	0.36	0.36	0.51	0.51
	H3	1.47	1.26	1.20	3.57	3.57
	L3	0.91	0.73	0.68	2.46	2.46
	C3	0.36	0.36	0.36	0.51	0.51
	H4	1.17	1.02	0.98	2.71	2.71
	L4	1.28	0.98	0.89	3.61	3.61
	C4	0.39	0.39	0.39	0.55	0.55
	H5	0.00	0.00	0.00	0.00	0.00
	L5	1.68	1.29	1.16	4.79	4.79
	C5	0.00	0.00	0.00	0.00	0.00
	H6	1.15	1.13	1.12	1.90	1.90
	L6	0.61	0.56	0.55	1.24	1.24
	C6	0.52	0.52	0.52	0.73	0.73
	H7	0.80	0.73	0.70	1.70	1.70
	L7	0.73	0.63	0.61	1.74	1.74
	C7	0.53	0.53	0.53	0.76	0.76
	H8	0.91	0.75	0.70	2.35	2.35
	L8	0.97	0.77	0.71	2.65	2.65
	C8	0.56	0.56	0.56	0.81	0.81
	H9	0.82	0.75	0.73	1.74	1.74
	L9	1.28	0.97	0.88	3.67	3.67
	C9	0.59	0.59	0.59	0.85	0.85
	H10	1.14	1.11	1.10	1.85	1.85
	L10	1.65	1.23	1.10	4.81	4.81
	C10	0.61	0.61	0.61	0.89	0.89
	H11	2.11	1.96	1.92	4.23	4.23.
	L11	0.94	0.82	0.78	2.23	2.23
	C11	0.86	0.85	0.85	1.20	1.20
	H12	0.89	0.86	0.86	1.47	1.47
	L12	0.99	0.84	0.80	2.46	2.46
	C12	0.81	0.80	0.80	1.15	1.15
	H13	0.00	0.00	0.00	0.00	0.00
	L13	1.15	0.91	0.84	3.14	3.14
	C13	0.85	0.85	0.85	1.23	1.23
	H14	0.87	0.85	0.84	1.43	1.43
	L14	1.42	1.07	0.96	4.09	4.09
	C14	0.88	0.88	0.88	1.28	1.28
	H15	2.04	1.90	1.86	4.03	4.03
	L15	1.75	1.30	1.16	5.08	5.08
	C15	0.93	0.93	0.92	1.34	1.34
Biases	1	0.40	0.23	0.16	1.35	1.35
	2	0.37	0.21	0.14	1.28	1.28
	3	0.39	0.22	0.15	1.36	1.36
	4	0.39	0.22	0.14	1.33	1.33
	5	0.38	0.21	0.14	1.30	1.30
	6	0.37	0.21	0.14	1.28	1.28

Low Altitude = 11 km.

6 Beams

Cols. 1-3 Δt = 5 sec.

Cols. 4-5 Δt = 10 sec.

Column	Number of Measurements Per Beam
1	370
2	370
3	370
4	185
5	185

Table 9 - Process Noise Checkout

		Process Noise Not Modelled	Modelled With Unreasonable Values
Stations	H2	1.51	1.51
	L2	0.77	0.77
	C2	0.51	0.51
	H3	1.89	1.90
	L3	1.13	1.13
	C3	0.51	0.51
	H4	1.53	1.53
	L4	1.55	1.55
	C4	0.55	0.55
	H5	0.00	0.00
	L5	2.05	2.05
	C5	0.00	0.00
	H6	1.62	1.62
	L6	0.82	0.82
	C6	0.73	0.73
	H7	1.07	1.07
	L7	0.95	0.95
	C7	0.75	0.75
	H8	1.15	1.15
	L8	1.20	1.20
	C8	0.79	0.79
	H9	1.11	1.11
	L9	1.54	1.54
	C9	0.83	0.83
	H10	1.60	1.60
	L10	1.98	1.98
	C10	0.87	0.87
	H11	2.88	2.88
	L11	1.23	1.23
	C11	1.20	1.20
	H12	1.24	1.24
	L12	1.28	1.28
	C12	1.13	1.14
	H13	0.00	0.00
	L13	1.43	1.43
	C13	1.21	1.21
	H14	1.21	1.21
	L14	1.70	1.70
	C14	1.25	1.25
	H15	2.76	2.76
	L15	2.08	2.09
	C15	1.32	1.32
Biases	1	0.43	0.43
	2	0.40	0.40
	3	0.42	0.42
	4	0.41	0.41
	5	0.40	0.40
	6	0.39	0.39

Low Altitude = 11 km.

6 Beams

Δt = 10 sec.

Column	Number of Measurements Per Beam
1	185
2	185

Table 10 - Process Noise

		Process Noise Not Modelled	Process Noise Modelled
Stations	H2	1.51	1.51
	L2	0.77	0.77
	C2	0.51	0.51
	H3	1.89	1.90
	L3	1.13	1.13
	C3	0.51	0.51
	H4	1.53	1.53
	L4	1.55	1.55
	C4	0.55	0.55
	H5	0.00	0.00
	L5	2.05	2.05
	C5	0.00	0.00
	H6	1.62	1.62
	L6	0.82	0.82
	C6	0.73	0.73
	H7	1.07	1.07
	L7	0.95	0.95
	C7	0.75	0.75
	H8	1.15	1.15
	L8	1.20	1.20
	C8	0.79	0.79
	H9	1.11	1.11
	L9	1.54	1.54
	C9	0.83	0.83
	H10	1.60	1.60
	L10	1.98	1.98
	C10	0.87	0.87
	H11	2.88	2.88
	L11	1.23	1.23
	C11	1.20	1.20
	H12	1.24	1.24
	L12	1.28	1.28
	C12	1.13	1.14
	H13	0.00	0.00
	L13	1.43	1.43
	C13	1.21	1.21
	H14	1.21	1.21
	L14	1.70	1.70
	C14	1.25	1.25
	H15	2.76	2.76
	L15	2.08	2.09
	C15	1.32	1.32
Biases	1	0.43	0.43
	2	0.40	0.40
	3	0.42	0.42
	4	0.41	0.41
	5	0.40	0.40
	6	0.39	0.39

Low Altitude = 11 km.

6 Beams

Δt = 10 sec.

Column	Number of Measurements Per Beam
1	185
2	180

Table 11 - Refraction

		1*	2* Noise Only	2* Unadjusted	3* Noise Only	3* Unadjusted	4*	5* Noise Only	5* Unadjusted
Stations	H2	1.51	1.51	0.28	1.62	0.18	1.16	1.16	0.31
	L2	0.77	0.77	0.14	0.79	0.12	0.59	0.59	0.15
	C2	0.51	0.51	0.03	0.54	0.04	0.36	0.36	0.02
	H3	1.89	1.90	0.39	2.03	0.31	1.47	1.47	0.43
	L3	1.13	1.13	0.29	1.18	0.27	0.91	0.91	0.32
	C3	0.51	0.51	0.02	0.59	0.03	0.36	0.36	0.02
	H4	1.53	1.53	0.31	1.67	0.24	1.17	1.17	0.34
	L4	1.55	1.55	0.45	1.58	0.44	1.28	1.28	0.49
	C4	0.55	0.55	0.02	0.57	0.02	0.39	0.39	0.02
	H5	0.00	0.00	0.00	0.00	0.00	0.00	0.00	0.00
	L5	2.05	2.05	0.60	2.08	0.61	1.68	1.68	0.65
	C5	0.00	0.00	0.00	0.00	0.00	0.00	0.00	0.00
	H6	1.62	1.62	0.23	1.62	0.19	1.15	1.15	0.23
	L6	0.82	0.82	0.11	0.82	0.13	0.61	0.61	0.12
	C6	0.73	0.73	0.04	0.78	0.04	0.52	0.52	0.04
	H7	1.07	1.07	0.10	1.06	0.07	0.80	0.80	0.12
	L7	0.95	0.95	0.12	0.92	0.18	0.73	0.73	0.14
	C7	0.75	0.75	0.01	0.74	0.04	0.53	0.53	0.02
	H8	1.15	1.15	0.27	1.27	0.22	0.91	0.91	0.30
	L8	1.20	1.20	0.29	1.25	0.30	0.97	0.97	0.32
	C8	0.79	0.79	0.03	0.79	0.02	0.56	0.56	0.03
	H9	1.11	1.11	0.16	1.13	0.16	0.82	0.82	0.19
	L9	1.54	1.54	0.47	1.60	0.46	1.28	1.28	0.51
	C9	0.83	0.83	0.04	0.80	0.01	0.59	0.59	0.04
	H10	1.60	1.60	0.16	1.69	0.05	1.14	1.14	0.16
	L10	1.98	1.98	0.63	2.06	0.61	1.65	1.65	0.67
	C10	0.87	0.87	0.01	0.86	0.02	0.61	0.61	0.02
	H11	2.88	2.88	0.55	3.00	0.44	2.11	2.11	0.55
	L11	1.23	1.23	0.22	1.27	0.27	0.94	0.94	0.24
	C11	1.20	1.20	0.08	1.23	0.07	0.86	0.86	0.07
	H12	1.24	1.24	0.16	1.35	0.14	0.89	0.89	0.16
	L12	1.28	1.28	0.23	1.25	0.30	0.99	0.99	0.27
	C12	1.13	1.14	0.05	1.20	0.07	0.81	0.81	0.04
	H13	0.00	0.00	0.00	0.00	0.00	0.00	0.00	0.00
	L13	1.43	1.43	0.33	1.46	0.39	1.15	1.15	0.37
	C13	1.21	1.21	0.03	1.26	0.06	0.85	0.85	0.04
	H14	1.21	1.21	0.09	1.34	0.03	0.87	0.87	0.10
	L14	1.70	1.70	0.50	1.78	0.52	1.42	1.42	0.54
	C14	1.25	1.25	0.04	1.28	0.04	0.88	0.88	0.04
	H15	2.76	2.76	0.37	3.10	0.24	2.04	2.04	0.38
	L15	2.08	2.09	0.63	2.21	0.68	1.75	1.75	0.68
	C15	1.32	1.32	0.04	1.38	0.04	0.93	0.93	0.04
Biases	1	0.43	0.43	0.02	0.39	0.00	0.40	0.40	0.03
	2	0.40	0.40	0.10	0.38	0.00	0.37	0.37	0.11
	3	0.42	0.42	0.01	0.39	0.00	0.39	0.39	0.02
	4	0.41	0.41	0.01	0.39	0.00	0.39	0.39	0.01
	5	0.40	0.40	0.01	0.39	0.01	0.38	0.38	0.00
	6	0.39	0.39	0.00	0.39	0.00	0.37	0.37	0.01

Low Altitude = 11 km.

6 Beams

Cols. 1-3 Δt = 10 sec.

Cols. 4-5 Δt = 5 sec.

Column	Number of Measurements Per Beam
1	185
2	185
3	185
4	370
5	370

1* Base Run - Refraction Not Considered

2* Base Run - Refraction Considered

3* Random Choose - Refraction Considered

4* Base Run - Refraction Not Considered

5* Base Run - Refraction Considered

Table 12 - Effect of Cross Passes

		No Cross Passes	4 Cross Passes
Stations	H2	1.51	1.31
	L2	0.77	0.69
	C2	0.51	0.42
	H3	1.90	1.65
	L3	1.13	1.00
	C3	0.51	0.44
	H4	1.53	1.35
	L4	1.55	1.38
	C4	0.55	0.46
	H5	0.00	0.00
	L5	2.05	1.81
	C5	0.00	0.00
	H6	1.62	1.38
	L6	0.82	0.73
	C6	0.73	0.62
	H7	1.07	0.90
	L7	0.95	0.81
	C7	0.75	0.63
	H8	1.15	0.99
	L8	1.20	1.05
	C8	0.79	0.68
	H9	1.11	0.94
	L9	1.54	1.38
	C9	0.83	0.68
	H10	1.60	1.39
	L10	1.98	1.76
	C10	0.87	0.75
	H11	2.88	2.43
	L11	1.23	1.08
	C11	1.20	0.98
	H12	1.24	1.04
	L12	1.28	1.09
	C12	1.14	0.96
	H13	0.00	0.00
	L13	1.43	1.24
	C13	1.21	1.02
	H14	1.21	1.01
	L14	1.70	1.51
	C14	1.25	1.06
	H15	2.76	2.34
	L15	2.09	1.85
	C15	1.32	1.13
Biases	1	0.43	0.41
	2	0.40	0.38
	3	0.42	0.40
	4	0.41	0.40
	5	0.40	0.39
	6	0.39	0.38

Low Altitude = 11 km.

6 Beams

Δt = 10 sec.

Column	Number of Measurements Per Beam
1	185
2	272

4.0 Conclusions

Figure 3.10-1 shows clearly that centimeter accuracy is achieved over 80 km baselines, even without exotic refraction equipment - such as two-color lasers.

It appears (Section 3.3) that the laser must be provided with six independent beams. Current investigations assume these to be individually steerable.

To minimize retroreflector cost while obtaining maximum grid extent, there appears to be an optimum aircraft low altitude between 11 km and 15 km and an associated retro spacing between 20 km and 27 km.

5.0 REFERENCES

Gibbs, B. G. and E. M. Haley, "Error Analysis of the Spacelab Geodynamics Laser Ranging System", Business and Technological Systems, Inc., BTS-TR-78-52, February 1978.

Appendix A

COMPUTATION OF A/C STATISTICS

The aircraft is assumed to be moving in a straight line during each pass, this is the reference trajectory. However, there are perturbations in the flight path which cannot be obtained from the onboard navigation or from GPS; these constitute the uncertainties in the aircraft position and velocity. We assume that these perturbations are generated by a second order system forced by white noise. Because these perturbations are deviations from the reference path, we assume that there is some control system which drives the aircraft back to the reference path. This provides a rationale for making the linear system asymptotically stable and thereby making the perturbation sequence stationary.

The model we have chosen is

$$\ddot{p} + 2\zeta\lambda\dot{p} + (\lambda^2+\nu^2)\, p = u$$

with

$$Eu = 0 \ , \ Eu(t)\, u(\tau) = q\delta(t-\tau) \ .$$

This model is physically inaccurate, since the perturbing accelerations, u , will not be white. However, we expect this to portray a satisfactory representation, on the basis that the combination of pilot/aircraft dynamics and atmospheric turbulence will generate a position sequence having this kind of correlation.

Initially, we shall presume that there are three independent Markov processes (x,y,z) with identical characteristics, while this may be unrealistic, it will be more realistic than the current procedure and will enable us to evaluate the benefits of this approach. In any case the program can be modified easily to provide for different characteristics.

$$\ddot{x} + 2\lambda\dot{x} + (\lambda^2+\nu^2)x = u$$

$$x = e^{-\lambda t}(c_1 \cos\nu t + c_2 \sin\nu t)$$

$$\dot{x} = e^{-\lambda t}\left[(-\lambda\cos\nu t - \nu\sin\nu t)c_1 + (\nu\cos\nu t - \lambda\sin\nu t)c_2\right]$$

OR

$$\begin{bmatrix} x \\ \dot{x} \end{bmatrix} = e^{-\lambda t}\begin{bmatrix} \cos\nu t & \sin\nu t \\ -(\lambda\cos\nu t + \nu\sin\nu t) & (\nu\cos\nu t - \lambda\sin\nu t) \end{bmatrix}\begin{bmatrix} c_1 \\ c_2 \end{bmatrix}$$

$$\begin{bmatrix} x_0 \\ \dot{x}_0 \end{bmatrix} = \begin{bmatrix} 1 & 0 \\ -\lambda & \nu \end{bmatrix}\begin{bmatrix} c_1 \\ c_2 \end{bmatrix}$$

$$\begin{bmatrix} c_1 \\ c_2 \end{bmatrix} = \begin{bmatrix} 1 & 0 \\ \frac{\lambda}{\nu} & \frac{1}{\nu} \end{bmatrix}\begin{bmatrix} x_0 \\ \dot{x}_0 \end{bmatrix}$$

$$\begin{bmatrix} x \\ \dot{x} \end{bmatrix} = e^{-\lambda t}\begin{bmatrix} (\cos\nu t + \frac{\lambda}{\nu}\sin\nu t) & \frac{1}{\nu}\sin\nu t \\ -\frac{(\lambda^2+\nu^2)}{\nu}\sin\nu t & (\cos\nu t - \frac{\lambda}{\nu}\sin\nu t) \end{bmatrix}\begin{bmatrix} x_0 \\ \dot{x}_0 \end{bmatrix}$$

$$X_{(2\times 1)} = \underline{\Phi}(t,t_0)\, X_{0\,(2\times 1)}$$

The program currently propagates the A/C covariance via the usual

$$P(t+\tau) = \phi P(t)\, \phi^T + Q\,, \qquad (1)$$

when $\lambda \neq 0$. When $\lambda = 0$, however,

$$p(t+\tau)_{A/C} = P_{oA/C}$$

where $P_{oA/C}$ is the initial aircraft covariance. In order to change this, we assume that x, y, and z each obeys a system

$$\frac{d}{dt}\begin{bmatrix} x \\ \dot{x} \end{bmatrix} = \begin{bmatrix} 0 & 1 \\ -(\lambda^2+\nu^2) & -2\lambda \end{bmatrix}\begin{bmatrix} x \\ \dot{x} \end{bmatrix} + \begin{bmatrix} 0 \\ 1 \end{bmatrix} u\,,$$

so that

$$\Phi = e^{-\lambda t}\begin{bmatrix} \cos \nu t + \frac{\lambda}{\nu} \sin \nu t & \frac{\sin \nu t}{\nu} \\ -\frac{\lambda^2+\nu^2}{\nu} \sin \nu t & \cos \nu t - \frac{\lambda}{\nu} \sin \nu t \end{bmatrix}$$

and

$$Q = \begin{bmatrix} q_{11} & q_{12} \\ q_{12} & q_{22} \end{bmatrix} q$$

where

$$q_{11} = \frac{1}{4\lambda(\lambda^2+\nu^2)} - \frac{e^{-2\lambda t}}{4\nu^2}\left[\frac{1}{\lambda} - \frac{\lambda \cos 2\nu t - \nu \sin 2\nu t}{\lambda^2+\nu^2}\right],$$

$$q_{12} = \frac{e^{-2\lambda\tau}}{4\nu^2}(1 - \cos 2\nu\tau)$$

$$q_{22} = \frac{1}{4\lambda} + \frac{e^{-2\lambda\tau}}{4\nu}\left[-\frac{\lambda^2+\nu^2}{\lambda\nu} + \frac{\lambda}{\nu}\cos 2\nu\tau + \sin 2\nu\tau\right],$$

and q is the spectral density of u.

In equilibrium $(t = \infty)$, we have

$$q_{11} = \frac{1}{4\lambda(\lambda^2+\nu^2)}$$

$$q_{12} = 0$$

$$q_{22} = \frac{1}{4\lambda}.$$

These values are derived in the appendix.

The parameter values have been selected to approximate A/C dynamic characteristics with

$$\lambda = \frac{1}{10 \text{ sec}}$$

and

$$\nu = \frac{2\pi}{30 \text{ sec}},$$

which gives

$$q_{11}(\infty) = 46.41$$

$$q_{12}(\infty) = 0$$

$$q_{22}(\infty) = 2.5.$$

We want the equilibrium value to have $q_{11} = 9E6 \text{ cm}^2$. Therefore

$q = 194000 \frac{cm^2}{sec^3}$ and $q_{22} = 485000 \frac{cm^2}{sec^4}$ $(696 \text{ cm/sec})^2$, a very large uncertainty.

The way this is handled in the computer, is that Q is computed for each step and the A/C uncertainty updated according to equation (1). Whenever a new track is started, however, the A/C uncertainty returns to P_o . To complicate matters, we have noticed in the past that when station uncertainties are small and A/C uncertainties are large then the matrix

$$[HPH^T + R] ,$$

appearing in the covariance update, is numerically singular. This occurs when the uncertainties in A/C position are so much larger than noise or station uncertainties that the matrix appears to have rank less than the number of beams. This difficulty has been handled by processing the measurements one at a time.

Appendix B
Covariance Matrix of a Second Order Markov Process

Consider the system

$$\dot{x} = \begin{bmatrix} 0 & 1 \\ -(\lambda^2+\nu^2) & -2\lambda \end{bmatrix} x + \begin{bmatrix} 0 \\ 1 \end{bmatrix} u \qquad (1)$$

associated with the equation

$$\ddot{x} + 2\lambda \dot{x} + (\lambda^2+\nu^2)\, x = u \,. \qquad (2)$$

The solution of this system is

$$x(t) = \Phi(t)x(0) + \int_0^t \Phi(t-s) \begin{bmatrix} 0 \\ 1 \end{bmatrix} u(s)ds \,, \qquad (3)$$

$$x(t) = \Phi(t)\, x\,(0) + w \,. \qquad (4)$$

If we take u to be a Gaussian random process, then it is reasonable to discuss the covariance of x. Let

$$E\, u(t) = 0 \,, \quad E\, u(t)u(\tau) = q\, \delta(t-\tau) \qquad (5)$$

where q is the (constant) spectral density of u, and define

$$P(t) = E\, x(t)\, x^T(t) \,. \qquad (6)$$

Then

$$P(t+\tau) = \Phi(\tau)\, P(t)\, \Phi^T(\tau) + Q(\tau)\, q \,. \qquad (7)$$

Explicitly,

$$\Phi(t) = e^{-\lambda t} \begin{bmatrix} \cos \lambda t \, \frac{\lambda}{\nu} \sin \nu t & \frac{\sin \nu t}{\nu} \\ -\frac{\lambda^2+\nu^2}{\nu} \sin \nu t & \cos t - \frac{\lambda}{\nu} \sin \nu t \end{bmatrix} . \qquad (8)$$

We now need to compute $Q(\tau)$,

$$Q(\tau) = E\, w(\tau)\, w^T(\tau)/q . \qquad (9)$$

This can be obtained directly from

$$w(\tau) = \int e^{-\lambda(\tau-s)} \begin{bmatrix} \frac{\sin \nu(\tau-s)}{\nu} \\ \cos \nu(\tau-s) - \frac{\lambda}{\nu} \sin \nu(\tau-s) \end{bmatrix} u(s)ds ; \qquad (10)$$

which comes from equation (3). Using (1) and (5) it is clear that $E\, w(\tau) = 0$; and

$$q_{11}(\tau) = \frac{1}{\nu^2} \int_0^\tau e^{-2\lambda(\tau-s)} \sin^2 \nu(\tau-s)\, ds , \qquad (11)$$

$$q_{12}(\tau) = \frac{1}{\nu} \int_0^\tau e^{-2\lambda(\tau-s)} \sin \nu(\tau-s) \cos \nu(\tau-s)\, ds - \lambda q_{11}(\tau) , \qquad (12)$$

and

$$q_{22}(\tau) = \int_0^\tau e^{-2\lambda(\tau-s)} \cos^2 \nu(\tau-s)\, ds - 2\lambda q_{12}(\tau) - \lambda^2 q_{11}(\tau) . \qquad (13)$$

These can be rewritten as

$$q_{11}(\tau) = \frac{1}{\nu^2} \int_0^\tau e^{-2\lambda s} \frac{1 - \cos 2\nu s}{2}\, ds ,$$

$$q_{12}(\tau) = \frac{1}{\nu} \int_0^\tau e^{-2\lambda s} \frac{\sin 2\nu s}{2} \, ds - \lambda q_{11}(\tau) ,$$

and

$$q_{22}(\tau) = \int_0^\tau e^{-2\lambda s} \frac{1 + \cos 2\nu s}{2} \, ds - 2\lambda q_{12}(\tau) - \lambda^2 q_{11}(\tau) ,$$

from which the values can be calculated:

$$q_{11}(\tau) = \frac{1}{4\lambda(\lambda^2+\nu^2)} - \frac{e^{-2\lambda\tau}}{4\nu} \left[\frac{1}{\lambda} - \frac{\lambda \cos 2\nu\tau - \nu \sin 2\nu\tau}{\lambda^2 + \nu^2} \right]$$

$$q_{12}(\tau) = \frac{1}{4(\lambda^2+\nu^2)} - \frac{e^{-2\lambda\tau}}{4\nu} \frac{\lambda \sin 2\nu\tau + \nu \cos 2\nu\tau}{\lambda^2 + \nu^2} - \lambda q_{11}(\tau)$$

$$= \frac{e^{-2\lambda\tau}}{4\nu^2} (1 - \cos 2\nu\tau) ,$$

$$q_{22}(\tau) = \frac{2\lambda^2+\nu^2}{4\lambda(\lambda^2+\nu^2)} - \frac{e^{-2\lambda\tau}}{4} \left[\frac{1}{\lambda} + \frac{\lambda \cos 2\nu\tau - \nu \sin 2\nu\tau}{\lambda^2 + \nu^2} \right]$$

$$- 2\lambda q_{12} - \lambda^2 q_{11} ,$$

$$= \frac{1}{4\lambda} + \frac{e^{-2\lambda\tau}}{4} \left[-\frac{\lambda^2+\nu^2}{\lambda\nu^2} + \frac{\lambda}{\nu^2} \cos 2\nu\tau + \frac{\sin 2\nu\tau}{\nu} \right] .$$

These formulae have been checked by verifying that

$$q_{11}(0) = 0 = q_{12}(0) = q_{22}(0)$$

and

$$\dot{q}_{11}(0) = 0 = \dot{q}_{12}(0) , \; \dot{q}_{22}(0) = 1 ,$$

which agrees with equations (11) - (13).